

Article

# Predicting Maize Transpiration, Water Use and Productivity for Developing Improved Supplemental Irrigation Schedules in Western Uruguay to Cope with Climate Variability

Luis Giménez <sup>1</sup>, Mário García Petillo <sup>2,†</sup>, Paula Paredes <sup>3,\*</sup> and Luis Santos Pereira <sup>3</sup>

<sup>1</sup> Departamento de Producción Vegetal, Facultad de Agronomía, Universidad de la República, Paysandú 60000, Uruguay; kapoexe@fagro.edu.uy

<sup>2</sup> Departamento de Suelos y Aguas, Facultad de Agronomía, Universidad de la República, Montevideo 12900, Uruguay; mgarciap@fagro.edu.uy

<sup>3</sup> LEAF—Landscape, Environment, Agriculture and Food, Institute of Agronomy, University of Lisbon, Lisbon 1349-017, Portugal; lspereira@isa.ulisboa.pt

\* Correspondence: pparedes@isa.ulisboa.pt; Tel.: +351-21-365-3339

† Dr. Mário García Petillo is deceased.

Academic Editor: Jerry Knox

Received: 28 April 2016; Accepted: 14 July 2016; Published: 22 July 2016

**Abstract:** Various maize irrigation treatments including full and deficit irrigation were used to calibrate and validate the soil water balance and irrigation scheduling model SIMDualKc at Paysandú, western Uruguay. The model adopts the dual crop coefficient approach to partition actual evapotranspiration ( $ET_{c,act}$ ) into actual transpiration ( $T_{c,act}$ ) and soil evaporation ( $E_s$ ). Low errors of estimation were obtained for simulating soil water content (Root mean square errors (RMSE)  $\leq 0.014 \text{ cm}^3 \cdot \text{cm}^{-3}$  with calibrated parameters, and  $RMSE \leq 0.023 \text{ cm}^3 \cdot \text{cm}^{-3}$  with default parameters). The ratio  $E_s/T_{c,act}$  ranged from 26% to 33% and  $E_s/ET_{c,act}$  varied from 20% to 25%, with higher values when the crop was stressed offering less soil coverage. Due to rainfall regime, runoff and deep percolation were quite large. The Stewarts phasic model was tested and used to predict maize yield from  $T_{c,act}$  with acceptable errors, in the range of those reported in literature. Water productivity values were high, ranging  $1.39$  to  $2.17 \text{ kg} \cdot \text{m}^{-3}$  and  $1.75$  to  $2.55 \text{ kg} \cdot \text{m}^{-3}$  when considering total water use and crop ET, respectively. Using a 22-year climatic data series, rainfed maize was assessed with poor results for nearly 40% of the years. Differently, alternative supplemental irrigation schedules assessed for the dry and very dry years have shown good results, particularly for mild deficit irrigation. Overall, results show appropriateness for using SIMDualKc to support the irrigation practice.

**Keywords:** dual crop coefficients; ET partitioning; SIMDualKc model; soil water balance; yield predictions; water scarcity and water saving

## 1. Introduction

Maize is a main summer crop in western Uruguay. In the last ten years, the cropped area increased by four times and that of maize by 2.5 [1]. That increase was made at the expenses of pasture and grassland. Maize production in Uruguay is constrained by water availability [2], which, as for the Argentinian pampas, is subject to large variability related with the El Niño Southern Oscillation (ENSO) [3]. Rainfed maize production largely varies due to a high variability of precipitation. Related adaptation measures include no-till systems [4,5] and supplemental irrigation since most of maize cropped area is rainfed [2].

In rainfed agriculture, mainly when soils have a small water storage capacity, it may not be possible to overcome impacts of the variability of rainfall as referred for maize [6]. Thus, it is important

to develop knowledge on maize water use in western Uruguay and to develop appropriate irrigation scheduling aimed at achieving the potential yields through efficient use of rainfall and irrigation water. A variety of factors influence irrigation management aimed at efficient use of water, improved water productivity and controlling environmental impacts [7–10]. The selection of appropriate supplemental irrigation scheduling options not only require knowledge of the time dynamics of crops demand for water but also adequate prediction of yield responses to water [11]. This justifies the use of models to develop strategies for supporting farmers' irrigation decision-making.

Numerous studies focused on the impacts of water stress on maize yields at various crop stages. Results of those studies (e.g., [12–14]) have shown that the most sensitive stages to water stress are emergence (VE stage), flowering which includes the tasseling and silking (VT and R1 stages), and early yield formation (R2 and R3 stages). Several approaches to assess the impacts of water deficits on yields have been developed. These include water–yield functions and crop growth and yield models. Applications of crop yield models to maize are numerous (e.g., [15–18]). However, these models are very demanding in terms of data and parameterization and may not be better than adopting a combination of a water balance simulation model with a water–yield function. Aiming at supporting irrigation scheduling, the Stewart's model [12,19–21] is largely used (e.g., [13,14] for maize). In recent years, the model was applied to a variety of crops [22–24] and maize [25–27]. Recently, that model was modified to relate yield with crop transpiration [28].

Numerous applications have been published on a variety of methods usable to optimize water and land allocation at basin and system levels [29–31], generally focusing multi-users and multi-crop systems. Differently, when focusing single crops, the search for more efficient water use is generally performed through simulation of alternative irrigation schedules which are compared through the respective impacts on total water use, yields and water productivity. With this purpose, both water balance simulation and crop–yield models may be used [6,32,33]. This approach was tested for maize using the soil water balance simulation model SIMDualKc [34], which partitions ET into soil evaporation ( $E_s$ ) and actual crop transpiration ( $T_{c\ act}$ ). Knowing  $T_{c\ act}$ , it is possible to adopt a water yield model based on impacts of transpiration deficits on yields to assess the performance of the studied irrigation schedules [28]. Considering the need for an optimal conjunctive use of rainfall and irrigation water, this approach may be particularly useful given the large rainfall variability observed during the maize crop season in western Uruguay.

Based upon maize field experiments adopting various irrigation strategies developed at Paysandú, western Uruguay, the objectives of this study consist of: (1) assessing the various components of maize water use with support of the SIMDualKc model; (2) predicting transpiration, yields and water productivity relative to various irrigation management strategies; (3) developing alternative supplemental irrigation schedules to improve rainfall and irrigation water use; and (4) assessing the performance of simulated irrigation strategies.

## 2. Materials and Methods

### 2.1. Site Characterization

Maize experiments were performed at the Experimental Station “Dr. M.A. Cassinoni” (32°22' S, 58°4' W, and 50 m elevation), at Paysandú, western Uruguay. According to the Köppen-Geiger classification [35], climate is a Cfa, warm temperate climate, with humid and hot summers. The average annual temperature is 18.3 °C and the average annual precipitation is 1327 mm, however with high inter-annual variability.

Weather data were collected with an automatic meteorological station (Vantage Pro 2TM, Davis Instruments, Hayward, CA, USA) located near the experimental fields. Maximum and minimum air temperature (°C), solar radiation ( $\text{MJ} \cdot \text{m}^{-2} \cdot \text{d}^{-1}$ ), wind speed ( $\text{m} \cdot \text{s}^{-1}$ ), air relative humidity (%), and precipitation (mm) were recorded daily; observations were performed above grass. These data were used to compute daily reference evapotranspiration ( $ET_0$ ) with the FAO-PM method [20]. Main climatic

data for both seasons relative to October 2011 to February 2012 and October 2012 to February 2013 are presented in Figure 1.

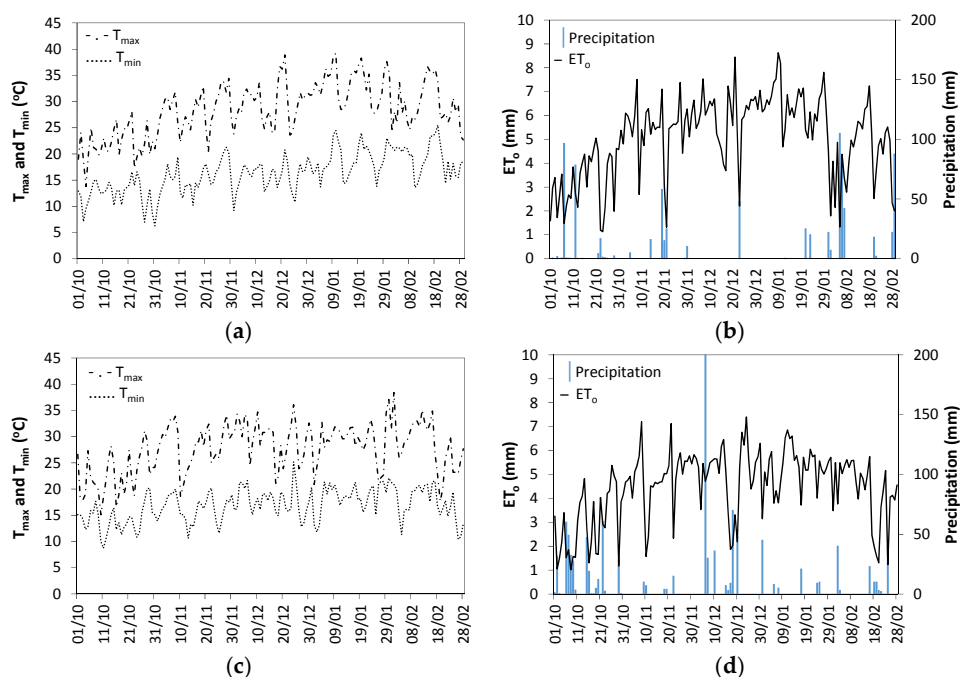


**Figure 1.** Daily weather data relative to the maize crop seasons of 2011–2012 (a,b) and 2012–2013 (c,d): maximum and minimum temperatures,  $T_{\max}$  and  $T_{\min}$  (a,c); precipitation and reference evapotranspiration ( $ET_o$ ) (b,d).

The soil is loamy in the first layer of 0.20 m and clay loamy thereafter. The main physical and hydraulic properties of the soil are presented in Table 1.

**Table 1.** Main soil physical and hydraulic properties of the experimental site, Paysandú.

Layer Depth (m)	Particle Size (%)			Soil Water Content ( $\text{cm}^3 \cdot \text{cm}^{-3}$ )	
	Sand	Silt	Clay	$\theta_{FC}$	$\theta_{WP}$
0–0.20	31.0	46.5	22.5	0.30	0.14
0.20–0.60	25.3	39.2	35.5	0.40	0.26
0.60–0.80	22.2	40.4	37.4	0.32	0.18

Note:  $\theta_{FC}$  and  $\theta_{WP}$  are respectively the soil water content at field capacity and wilting point.

Crop management was the same as recommended in the area to be adopted by local farmers. Plots cropped with maize were monitored to assess different irrigation schedules. The irrigation system consisted of pressure compensating in-line drippers spaced 0.20 m along the lateral; the operating pressure was 98 kPa; and the emitters discharge was  $1.49 \text{ L} \cdot \text{h}^{-1}$ . Drip lines were located between every pair of crop rows, which were spaced by 0.70 m. Evaluations of the distribution uniformity (DU) of water applications were performed; an average  $DU = 90\%$  was observed. Irrigation depths were measured with a flowmeter installed upstream of each plot. Soil water content (SWC) was measured with a calibrated neutron probe (503DR HYDROPROBE, InstroTek Inc., Martinez, CA, USA). Measurements were performed at each 0.10 m until a maximum of 0.80 m. However, considering the inappropriateness of using neutron probes in the surface soil layer [36], SWC was determined in the upper 0.10 m layer through soil sampling followed by oven drying.

The following irrigation strategies were adopted in the crop season of 2012–2013:

- FI, full irrigation, aimed at minimizing water stress in all crop growth stages;

- $DI_{FLO}$ , deficit irrigation from end flowering to the late reproductive stage (1–28 January 2013);
- $DI_{MAT}$ , deficit irrigation during the maturation period (1–10 February 2013);
- $DI_{VEG+REP}$ , deficit irrigation during the vegetative and the reproductive stages (15 November–5 December 2012 and 5–28 January 2013); and
- Rainfed.

Irrigations were scheduled using a simplified daily soil water balance applied to the effective root zone depth  $Z_r = 0.75$  m and using the observed weather and SWC data. Irrigation depths were set to refill SWC up to 90% of  $\theta_{FC}$  in the periods when water stress was not allowed and up to 60% of  $\theta_{FC}$  otherwise. Irrigation were applied whenever a depletion of 60% of the total available soil water (TAW, mm) was attained for the periods when aiming at inducing water stress. Otherwise, irrigations were applied when a depletion of 40% of TAW was reached. TAW was defined as  $TAW = (\theta_{FC} - \theta_{WP}) 1000 Z_r$ . No stress was allowed during emergence in order to assure a good crop establishment.

Water deficits during the targeted periods referred above were induced by withholding irrigation and preventing rainfall with a shelter that was moved to cover the plots when rainfall occurred. The experimental design consisted in completely random blocks with three replications of the above referred five irrigation strategies. Experimental plots were 3.5 m  $\times$  5 m, similar to those used by Echarte et al. [37] when assessing maize sowing densities for the region. The 1.5 m wide strips bordering the plots were also planted with maize to control advection effects, thus minimizing effects of plot sizes. It resulted that the continuous area cropped with maize totalized 352.5 m<sup>2</sup>. The irrigation schedules applied are described in Table 2.

**Table 2.** Irrigation dates and depths for all treatments and both season.

Treatments					
2011–2012		2012–2013		2012–2013	
Calibration ( $DI_{FLO}$ )		FI		$DI_{FLO}$	
Dates	Depths (mm)	Dates	Depths (mm)	Dates	Depths (mm)
11 November	11	7 November	12	7 November	12
18 November	7	9 November	16	9 November	16
28 November	16	17 November	16	17 November	16
21 December	16	24 November	16	24 November	16
6 December	16	1 December	19	01 December	19
10 December	16	14 December	16	14 December	16
14 December	25	17 December	7	28 January	25
19 December	25	26 December	16	29 January	25
30 December	25	29 December	25	8 February	25
1 January	25	31 December	25	11 February	25
3 January	16	9 January	25		
5 January	25	14 January	25		
13 January	25	21 January	25		
30 January	25	3 January	25		
		11 February	25		
Treatments 2012–2013					
$DI_{MAT}$		$DI_{VEG-REP}$		Rainfed	
Dates	Depths (mm)	Dates	Depths (mm)	Dates	Depths (mm)
7 November	12	7 November	12	7 November *	12
9 November	16	9 November	16	9 November *	16
17 November	16	17 November	16		
24 November	16	26 December	25		
01 December	19	28 January	25		
14 December	16	29 January	25		
26 December	16	8 February	25		
29 December	25	11 February	25		
30 December	25				
9 January	25				
14 January	25				
11 February	25				

Note: \* Irrigations performed to avoid stress during plant emergence.

The maize hybrid DK 692 was selected as recommended by the Uruguayan National Cultivars Evaluation System adopting a plant density of 100,000 plants·ha<sup>-1</sup>, which is commonly adopted in the region following the studies by Echarte et al. [37]. Densities larger than 80,000 plants·ha<sup>-1</sup> are commonly used in Europe and in China [28,34,38] but vary with the variety used. The dates of each crop growth stages as proposed in FAO56 [20] and the cumulated growing degree days (CGDD) are presented in Table 3. The crop height (h, m) and the fraction of soil covered by the canopy ( $f_c$ , dimensionless) are given in Table 4.  $f_c$  along the crop seasons were visually estimated as the percentage of soil shaded by the crop near solar noon. Rooting depths ( $Z_r$ , m) were measured in randomly distributed plants throughout the season, and this surveillance was performed collecting soil samples with an Edelman type probe (Eijkelkamp, NL, USA) to a depth of 1.0 m and visually checking for the existence of roots at each 0.10 m depth. The maximum root depth observed was 0.75 m, with most of the roots in the first 0.30 to 0.40 m of soil.

Biomass and grain yield were obtained when harvesting all experimental plots and standard deviations were computed; samples were oven dried to constant weight at  $65 \pm 5$  °C and the yield was adjusted and measured at 13.5% grain moisture.

**Table 3.** Crop growth stages dates and accumulated growth degree days (CGDD) for each experimental season.

Treatment	Year	Data	Crop Growth Stages			
			Initial Period	Crop Development	Mid-Season	Late-Season
Calibration	2011–2012	Initial date	27 October	15 November	18 December	29 January
		End date	14 November	17 December	28 January	28 February
		CGDD (°C)	207	668	1320	1826
FI	2012–2013	Initial date	25 October	8 November	10 December	1 February
		End date	7 November	9 December	31 January	28 February
		CGDD (°C)	200	640	1442	1858
DI <sub>FLO</sub>	2012–2013	Initial date	25 October	8 November	12 December	25 January
		End date	7 November	11 December	24 January	28 February
		CGDD (°C)	200	672	1336	1858
DI <sub>MAT</sub>	2012–2013	Initial date	25 October	8 November	12 December	22 January
		End date	7 November	11 December	21 January	22 February
		CGDD (°C)	200	672	1288	1788
DI <sub>VEG-REP</sub>	2012–2013	Initial date	25 October	8 November	10 December	29 January
		End date	7 November	9 December	28 January	28 February
		CGDD (°C)	200	640	1393	1858
Rainfed	2012–2013	Initial date	25 October	8 November	10 December	15 January
		End date	7 November	9 December	14 January	5 February
		CGDD (°C)	200	640	1177	1531

**Table 4.** Crop height (h) and fraction of ground covered by the crop ( $f_c$ ) at the main crop growth stages.

Year and Treatment	Data	Crop Growth Stages				
		Sowing	Start of Crop Development	Start of Mid-Season	Start of Late-Season	Harvest
2011–2012	h (m)	0	0.18	1.80	2.00	1.95
	$f_c$	0.01	0.10	0.80	0.90	0.85
2012–2013	h (m)	0	0.25	1.85	2.00	1.97
	$f_c$	0.01	0.10	0.83	0.95	0.90
DI <sub>FLO</sub>	h (m)	0	0.20	1.70	1.75	1.70
	$f_c$	0.01	0.10	0.75	0.70	0.65
DI <sub>MAT</sub>	h (m)	0	0.20	1.92	2.00	1.95
	$f_c$	0.01	0.10	0.85	0.90	0.90
DI <sub>VEG-REP</sub>	h (m)	0	0.20	1.65	1.75	1.67
	$f_c$	0.01	0.10	0.75	0.85	0.80
Rainfed	h (m)	0	0.22	1.60	1.75	1.71
	$f_c$	0.01	0.10	0.70	0.70	0.65

### 2.2. Modeling

The modeling strategy used in the present study consists of combining the soil water balance model SIMDualKc [34], which simulates water use and crop evapotranspiration, with the global (S1) and the multi-phasic (S2) water–yield models [12,19] as shown in the flow chart of Figure 2.

The SIMDualKc model performs a daily soil water balance at field scale, thus computing the water use components of a crop, particularly plant transpiration and soil evaporation using the dual crop coefficient approach (dual  $K_c$ ) [20,39]. The model is appropriate to generate irrigation scheduling alternatives and to support farm irrigation scheduling. The model performance has been assessed relative to its capability to simulate soil evaporation and plant transpiration (e.g., [38,40,41]). The adequateness of the dual  $K_c$  approach has been independently assessed [42,43].

The model computes potential crop evapotranspiration ( $ET_c$ , mm) as

$$ET_c = (K_{cb} + K_e) ET_o \tag{1}$$

where  $ET_o$  is reference evapotranspiration (mm),  $K_{cb}$  is the basal crop coefficient (dimensionless) that characterizes crop transpiration and  $K_e$  is the evaporation coefficient (dimensionless) characterizing soil evaporation. Therefore, the model computes separately crop transpiration  $T_c = K_{cb} ET_o$  and soil evaporation  $E_s = K_e ET_o$ . The terms and parameters in Equation (1) refer to potential crop evapotranspiration, which occurs when the crop is non-stressed and able to attain maximum yield. Otherwise, the actual ET ( $ET_{c\ act}$ , mm) is computed as a function of the available soil water in the root zone.

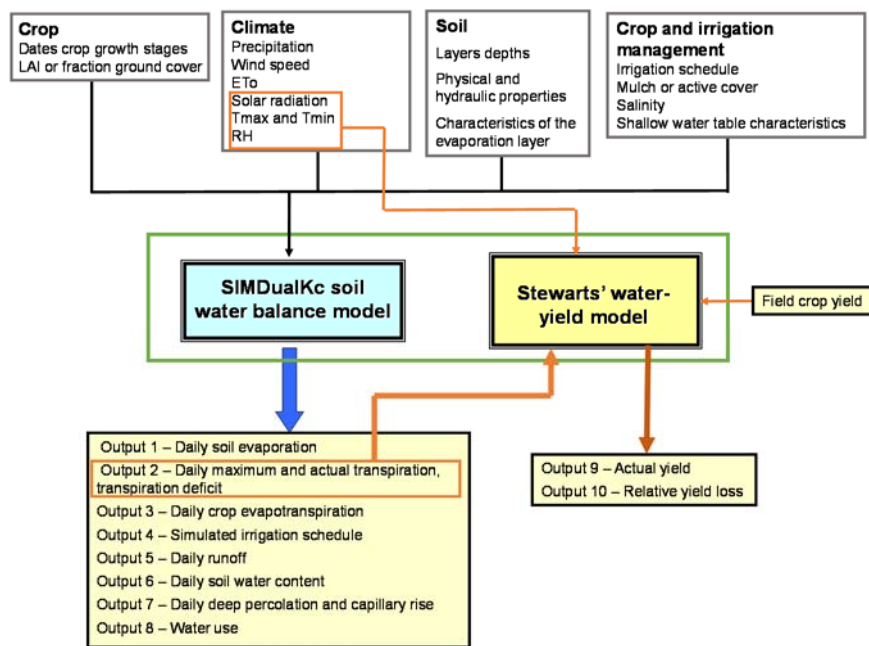


**Figure 2.** Flow-chart for the simplified approach combining the soil water balance model SIMDualKc with the Stewart’s water–yield model.

The total available soil water (TAW, mm) is defined as the soil water storage in the root zone between field capacity ( $\theta_{FC}$ ,  $cm^3 \cdot cm^{-3}$ ) and the wilting point ( $\theta_{WP}$ ,  $cm^3 \cdot cm^{-3}$ ). The readily available soil water (RAW, mm) is  $RAW = p TAW$  where  $p$  is the soil water depletion fraction for no stress. Water stress occurs when the available soil water content (ASW, mm) is below the threshold RAW. ASW is computed from the actual soil water content (SWC,  $cm^3 \cdot cm^{-3}$ ) as  $ASW = (SWC - \theta_{WP}) 1000 Z_r$ . Water stress is expressed through the stress coefficient ( $K_s$ , 0–1) defined [20,39] as a function of the depletion in the effective root zone ( $D_r$ ):

$$K_s = \frac{TAW - D_r}{TAW - RAW} = \frac{TAW - D_r}{(1 - p) TAW} \quad (2)$$

with  $K_s = 1$  for  $D_r \leq RAW$ .

$ET_{c \text{ act}}$  equals  $ET_c$  when  $K_s = 1$ . Differently,  $ET_{c \text{ act}} < ET_c$  when  $K_s < 1.0$ , with  $ET_{c \text{ act}}$  given by

$$ET_{c \text{ act}} = (K_s K_{cb} + K_e) ET_o \quad (3)$$

Under these conditions, the actual plant transpiration is  $T_{c \text{ act}} = K_s K_{cb} ET_o$ , thus depending upon  $K_s$ . When stress affects crop growth and the coverage of the ground by the crop canopy  $K_e$  also changes.  $K_e$  is computed through a daily water balance of the evaporation soil layer, which is characterized by its depth ( $Z_e$ , m), the total evaporable water (TEW, mm) and the readily evaporable water (REW, mm). TEW is the maximum depth of water that can be evaporated from the evaporation soil layer when it has been completely wetted, and REW is the depth of water that can be evaporated without water availability restrictions [20,39]. The model computes the soil water balance in the root zone in terms of depletion at the end of every day [20,44]:

$$D_{r,i} = D_{r,i-1} - (P - RO)_i - I_i - CR_i + ET_{c \text{ act},i} + DP_i \quad (4)$$

where  $D_{r,i}$  and  $D_{r,i-1}$  are the root zone depletion (mm) at the end of, respectively, Day  $i$  and Day  $i-1$ ,  $P$  is precipitation (mm),  $RO$  is runoff (mm),  $I$  is net irrigation depth (mm),  $CR$  is capillary rise from a shallow groundwater table (mm),  $ET_{c \text{ act}}$  is the actual evapotranspiration (mm), and  $DP$  is deep percolation (mm), all terms referring to Day  $i$ .  $RO$  is computed using the curve number approach [45].  $CR$  was not considered in this study because the water table depth was below 10 m.  $DP$  fluxes were computed with the decay parametric equation proposed by Liu et al. [46], which relates the soil water stored after occurrence of a heavy rain or irrigation ( $W_a$ , mm) with the time  $t$  (days) to attain field capacity. In that function, the parameter  $a_D$  (mm) characterizes storage and  $b_D$  refers to velocity of vertical drainage; both parameters depend upon the soil physical characteristics [46].

Irrigation scheduling options available in SIMDualKc are based upon the concepts of depletion fraction for no stress ( $p$ ), management allowed depletion (MAD), TAW and RAW. Those options include: (1) irrigation to prevent water stress, when  $MAD \leq p$ ; (2) deficit irrigation, when  $MAD > p$ , i.e., the available soil water may be depleted to a threshold level below RAW; (3) user selected irrigation depths and intervals between irrigation events; and (4) no irrigation [34]. Furthermore, the computation of the seasonal net irrigation requirements (NIR, mm) as defined by Doorenbos and Pruitt [47] is also available.

The SIMDualKc model requires calibration when used with a crop different of those previous simulated, or, for the same crop, in a different environmental and managerial context as recently discussed [48,49]. Calibration focuses on the crop parameters  $K_{cb}$  and  $p$ , the soil evaporation parameters  $Z_e$ , TEW and REW, and the  $RO$  and  $DP$  parameters. Otherwise, default parameters can be used because errors are small when using well selected default parameters [45,50]; thus, the parameters obtained for the calibration at Paysandú should be further used as default in other locations of western Uruguay.

In the present study, aiming at assessing irrigation scheduling impacts on yields, the SIMDualKc model was combined with the water–yield models S1 and S2 proposed by Stewart et al. [12]. The model approach S1 assumes a linear relationship between the relative yield loss,  $RYL = 1 - Y_a/Y_m$ , and the relative evapotranspiration deficit,  $RED = 1 - ET_{c \text{ act}}/ET_c$ . The modified approach [28] consists of adopting a relative transpiration deficit (RTD) instead of RED. This approach is justified because transpiration is the ET component directly responsible for yield formation [51] and, therefore, several crop growth models used  $T_{c \text{ act}}$  for the estimation of biomass and yield [21,52]. Thus, the S1 model predicts actual yields as:

$$\hat{Y}_a = Y_m - \frac{Y_m K_y T_d}{T_c} \quad (5)$$

where  $Y_m$  is maximum (potential) yield ( $\text{kg} \cdot \text{ha}^{-1}$ ),  $T_d$  is the seasonal transpiration deficit (mm), with  $T_d = T_c - T_{c\text{act}}$  and  $K_y$  is the yield response factor (dimensionless). The  $Y_a$  values observed at the experimental plots of Paysandú from 2010–2011 to 2012–2013 combined with the modeled  $T_d$  were used to obtain the  $K_y$  as previously proposed [28]. The  $Y_m$  values were obtained from the highest yields achieved for the non-stressed treatments and from yield data information collected from farmers in the study area, however adjusted to climate conditions using the “Wageningen method” [19]. This method uses data on the seasonal shortwave radiation, saturation vapor pressure deficit,  $ET_c$  and the duration of the crop cycle.  $Y_m$  was  $15.7 \text{ t} \cdot \text{ha}^{-1}$  for 2011–2012;  $14.2 \text{ t} \cdot \text{ha}^{-1}$  in 2012–2013 for FI,  $DI_{\text{FLO}}$  and  $DI_{\text{VEG-REP}}$ . Because harvesting was anticipated for  $DI_{\text{MAT}}$  and rainfed cases, it resulted a smaller  $Y_m = 11.9 \text{ t} \cdot \text{ha}^{-1}$  (Table 3).

The S2 model was also modified to consider  $T_{c\text{act}}$  [28] and takes into consideration the time periods when water stress occurs, which is particularly important for maize due to its sensitivity to water stress, particularly at flowering and yield formation [12]. The S2 model uses a three parameters function:

$$\hat{Y}_a = Y_m - \frac{Y_m (\beta_v T_{d,v} + \beta_f T_{d,f} + \beta_m T_{d,m})}{T_c} \quad (6)$$

where  $\beta_v$ ,  $\beta_f$  and  $\beta_m$  are the yield response factors (dimensionless) relative to the vegetative growth period (VE to V10 stages), the flowering (pollination) period, from first tassel until blister kernel (VT to R2 stages), and the maturation period, from milk stage until physiological maturity (R3 to R6 stages).  $T_{d,v}$ ,  $T_{d,f}$  and  $T_{d,m}$  are the transpiration deficits (mm) for the same crop periods. The parameters  $\beta_v$ ,  $\beta_f$  and  $\beta_m$  used in the present study were those proposed by Alves et al. [53], respectively, 1.2, 2.8 and 0.9, when the crop was conditioned by water deficits during the vegetative growth period, otherwise,  $\beta_v = 2.1$ ,  $\beta_f = 7.9$  and  $\beta_m = 2.1$  [53]. The S2 model was also tested using all observed  $Y_a$  data during 2010–2011, 2011–2012 and 2012–2013 as well as the model computed  $T_d$ .

### 2.3. Calibration and Validation Procedures

Model calibration is the process of adjusting influential model parameters within their reasonable ranges aiming at achieving the best fit of observed SWC by the simulated SWC as discussed by Pereira et al. [49]. Model calibration consisted therefore in searching the parameters relative to the crop ( $K_{cb}$ ,  $p$ ), the soil evaporation layer ( $Z_e$ , TEW, REW), runoff (CN) and deep percolation ( $a_D$  and  $b_D$ ) that lead to minimal deviations between the simulated and observed SWC values. Model validation consisted in evaluating the accuracy of the model when the calibrated parameters are used to simulate independent observed data sets. Calibration was performed using the  $DI_{\text{FLO}}$  data set of 2011–2012, which was selected because its completeness of SWC data, and validation was performed for all five irrigation treatments of 2012–2013.

The calibration was performed through an iterative trial and error procedure of searching the best parameters values, first through visualizing the decrease of deviations between observed and simulated SWC values, later by observing when the root mean square errors were decreasing until nearly stabilizing. The trial and error procedure was applied by steps because the number of searched parameters is large. It was first applied to the  $K_{cb}$  and  $p$  values, then to the runoff (RO), deep percolation (DP) and soil evaporation parameters, lately to the crop parameters again and finally considering all parameters. The search was performed considering the expected range of variation of the parameter values.

The initial values for  $K_{cb}$  and  $p$  were those tabled by Allen et al. [20], for soil evaporation were those based on values proposed by Allen et al. [39], for RO were those based on CN values proposed by Allen et al. [45], and the initial DP parameters were those proposed by Liu et al. [46] for loamy soils. The water balance was initialized two days prior to sowing when SWC observations were performed. In 2011–2012, the initial soil water depletion in the surface layer ( $D_e$ ) was null and the SWC in the underneath layers was 7% above field capacity. For 2012–2013, the initial  $D_e$  was null and  $D_r$  was also null for treatments  $DI_{\text{MAT}}$ ,  $DI_{\text{VEG-REP}}$  and rainfed, while  $D_e$  was 20% of TEW and  $D_r$  was 15% of TAW for FI and  $DI_{\text{FLO}}$ . Differences between treatments relate with soil water holding characteristics of the plots.

“Goodness-of-fit” indicators were used to assess the performance of SIMDualKc at calibration and validation. The adopted indicators were computed from the pairs of observed and predicted SWC values, respectively  $O_i$  and  $P_i$  ( $i = 1, 2, \dots, n$ ), whose means are, respectively,  $\bar{O}$  and  $\bar{P}$ . Following previous SIMDualKc applications [48,49] and Legates and McCabe Jr. [54], the indicators are:

- i The regression coefficient  $b_0$  of a regression forced to the origin (FTO) relating  $O_i$  and  $P_i$  SWC values, which aim at recognizing how similar were the simulated and observed values, computed as

$$b_0 = \frac{\sum_{i=1}^n O_i P_i}{\sum_{i=1}^n O_i^2} \quad (7)$$

- ii The determination coefficient of the ordinary least squares regression of the same variables aimed at assessing the fraction of the variance of observations that was explained by the model.

$$R^2 = \left\{ \frac{\sum_{i=1}^n (O_i - \bar{O}) (P_i - \bar{P})}{\sqrt{\sum_{i=1}^n (O_i - \bar{O})^2} \sqrt{\sum_{i=1}^n (P_i - \bar{P})^2}} \right\}^2 \quad (8)$$

- iii The root mean square error (RMSE), which expresses the variance of the residual errors, computed as

$$\text{RMSE} = \sqrt{\frac{\sum_{i=1}^n (O_i - P_i)^2}{n}} \quad (9)$$

which may vary between 0.0, when a perfect match would occur, and a positive value, which should be smaller than the mean of observations.

- iv The normalized RMSE (NRMSE), that is defined as the ratio between RMSE and the observations mean  $\bar{O}$ , which expedites the comparison of its values for different variables, computed as

$$\text{NRMSE} = \frac{\text{RMSE}}{\bar{O}} \quad (10)$$

- v The average relative error (ARE), that expresses the estimation errors as a percentage of observation values

$$\text{ARE} = \frac{100}{n} \sum_{i=1}^n \left| \frac{O_i - P_i}{O_i} \right| \quad (11)$$

- vi The Nash and Sutcliff [55] modeling efficiency (EF), which expresses the relative magnitude of the mean square error ( $\text{MSE} = \text{RMSE}^2$ ) when compared with the observed data variance [52]:

$$\text{EF} = 1.0 - \frac{\sum_{i=1}^n (O_i - P_i)^2}{\sum_{i=1}^n (O_i - \bar{O})^2} \quad (12)$$

$\text{EF} = 1$  is the target value and values close to 1.0 indicate that the model performance is very good since then the mean square error is much smaller than the variance of observations. Contrarily, when EF is null or negative, this means that there is no gain in using the model.

The same indicators were used when testing the water–yield parameters of Equations (5) and (6).

#### 2.4. Generating and Assessing Alternative Supplemental Irrigation Scenarios

Using a 22-year series of weather variables provided by the Uruguayan Meteorological Institute (INUMET), a series of NIR values was obtained with SIMDualKc. Adopting an empirical frequency distribution for the NIR series, it was possible to characterize the climatic demand and selecting the years when the probabilities of NIR exceedance were 20% and 5%, which correspond to dry and very dry conditions [6].

For both the dry and very dry years, supplemental irrigation scheduling (SIS) alternatives were set with SIMDualKc, which was used to design various SIS, including full and deficit irrigation (DI). These SIS are different from the irrigation strategies used in the field trials because the latter aimed at assessing the impacts on yield of water stress imposed at selected crop growth stages while the SIS are aimed at searching alternative schedules leading to improved water use and productivity. The DI schedules were designed to control water stress during the most sensitive crop stages—germination/emergence, flowering/pollination, and maturation—therefore to minimize water stress impacts on yields. Simulations were performed considering the average CGDD as indicated in Table 3. The various SIS were built with fixed net irrigation depths ( $D = 30$  mm) as proposed by García-Petillo [56], and ceasing irrigation 20 days before harvesting. A similar  $D$  was adopted by Martins et al. [57]. The MAD irrigation thresholds were:

- i Full irrigation (Full), aimed at preventing water stress, with  $MAD = p$ .
- ii Mild deficit irrigation (Mild):  $MAD = 1.20 p$  for the initial period,  $MAD = 1.30 p$  for the crop development and the late season periods, and  $MAD = 1.10 p$  during mid-season, which includes flowering and yield formation.
- iii Moderate deficit irrigation (Mod) with  $MAD = 1.30 p$  for the initial and crop development periods,  $MAD = 1.20 p$  for the mid-season period, and  $MAD = 1.40 p$  for the late-season, after grain filling until harvesting.
- iv Rainfed.

The performances of the SIS and rainfed scenarios were assessed using various indicators: total water use (TWU), relative yield decrease (RYD) and water productivity (WP). The latter was computed [8] as the ratio between the predicted actual yield and the seasonal TWU computed as

$$TWU = P_e + GI + \Delta ASW \quad (13)$$

where  $P_e$  is effective precipitation (mm), i.e., the difference between total precipitation and runoff,  $GI$  is gross irrigation (mm), and  $\Delta ASW$  is the variation of the available soil water (mm) between planting and harvesting, positive when  $ASW(\text{harvesting}) < ASW(\text{planting})$ . In addition, following Pereira et al. [8], the consumptive use  $WP$  ( $WP_{ET}$ ), often called water use efficiency, which is the ratio between the actual yield and the actual crop evapotranspiration, was also computed.

### 3. Results and Discussion

#### 3.1. Soil Water Balance Modeling and Model Parameterization

The calibration and validation of SIMDualKc through comparing predicted and observed SWC was the main modeling issue. Results relative to the calibration and two validation cases are shown in Figure 3 when using both calibrated and default parameters.

Analyzing Figure 3, it can be noticed that water stress occurred in the deficit irrigation case used for calibration (Figure 3a,b) and for the rainfed case used for validation (Figure 3e,f), respectively, from 10 to 30 January 2012 and from 13 January to 1 February 2013. Differently, no water stress occurred for the full irrigation case.

The “goodness-of-fit” indicators relative to all simulated cases using calibrated or default parameters are presented in Table 5. Regression coefficients for all treatments are very close to 1.0, therefore indicating that the predicted SWC values are statistically close to the observed ones. The values of the determination coefficients are generally close to 0.90, varying from 0.76 to 0.95, thus showing that most of the variance is explained by the model. Naturally, the indicators referring to the use of calibrated parameters are superior to those relative to using default parameters. The errors of estimate are small, with  $RMSE \leq 0.014 \text{ cm}^3 \cdot \text{cm}^{-3}$  when calibrated parameters were used, and  $\leq 0.023 \text{ cm}^3 \cdot \text{cm}^{-3}$  when default parameters were used. The corresponding normalized values NRMSE are also quite small, not exceeding 0.07; similarly, ARE did not exceed 3.4% and 6.7%, respectively,

when parameters used were calibrated or default. EF ranged from 0.71 to 0.87 when calibrated parameters were used, thus indicating that the mean square error was much smaller than the measured data variance. Moreover, lower but reasonably high EF values were also obtained when using default parameters. Overall, results in Figure 3 and Table 5 show that the model is appropriate for use in western Uruguay for applications aimed at supporting improved irrigation practices and management, including when adopting default parameters if these are well selected.

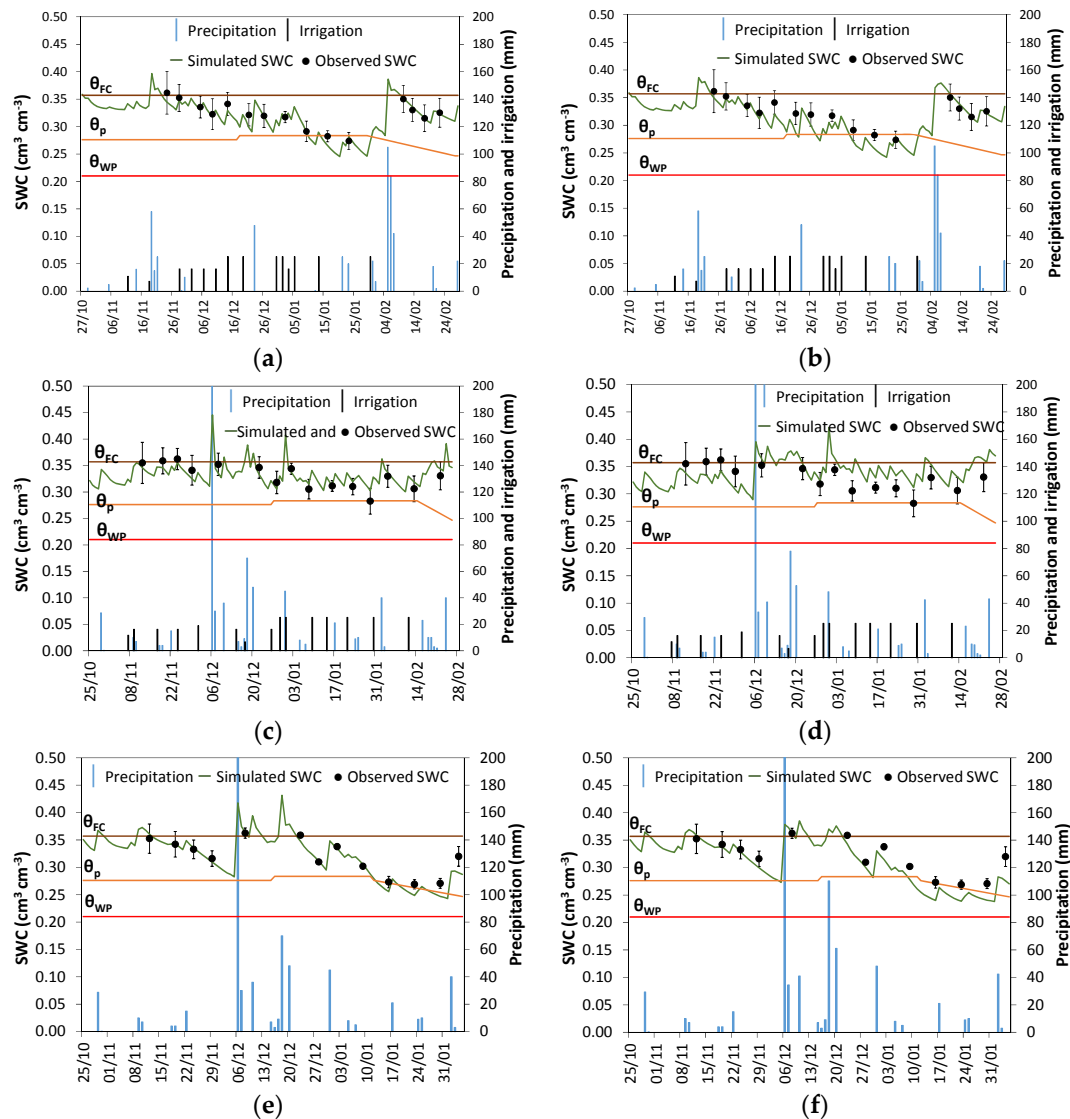


**Figure 3.** Simulated vs. observed seasonal variation of soil water content (SWC,  $\text{cm}^3 \cdot \text{cm}^{-3}$ ) when using calibrated (left) and default parameters (right): a deficit irrigation case for 2011–2012 used for calibration (a,b); FI in 2012–2013 (c,d) and rainfed in 2012–2013 (e,f), both used for validation. ( $\theta_{FC}$  and  $\theta_{WP}$  represent SWC at field capacity and wilting point, and  $\theta_p$  is the SWC threshold for no stress; error bars represent the standard deviation of the SWC measurements). Also depicted precipitation and irrigation.

The default (initial) and calibrated model parameters—basal crop coefficients, depletion fractions for no stress, and parameters relative to soil evaporation, runoff and deep percolation—are presented in Table 6. It can be noted that differences between default and calibrated parameters are small (Table 6) because default parameters were well selected and resulted close to the calibrated ones, which is a main reason for the small errors obtained when using default parameters (Table 5).

**Table 5.** Indicators of “goodness-of-fit” of SIMDualKc model applied to all treatments when using calibrated and default parameters.

		$b_0$	$R^2$	RMSE ( $\text{cm}^3 \cdot \text{cm}^{-3}$ )	NRMSE	ARE (%)	EF
Calibrated parameters	2011–2012, (calibration)	0.98	0.88	0.010	0.03	2.2	0.84
	2012–2013 (validation)						
	FI	0.99	0.76	0.012	0.04	3.4	0.71
	DI <sub>FLO</sub>	1.00	0.95	0.012	0.04	2.8	0.80
	DI <sub>MAT</sub>	1.01	0.89	0.012	0.04	2.8	0.87
	DI <sub>VEG-FLO</sub>	0.98	0.92	0.013	0.04	3.3	0.76
	Rainfed	0.98	0.94	0.014	0.04	3.3	0.81
Default parameters	2011–2012	0.97	0.82	0.017	0.05	4.3	0.53
	2012–2013						
	FI	1.02	0.21	0.023	0.07	6.7	−0.03
	DI <sub>FLO</sub>	0.99	0.95	0.015	0.05	4.0	0.70
	DI <sub>MAT</sub>	1.01	0.87	0.014	0.04	3.4	0.82
	DI <sub>VEG-FLO</sub>	0.97	0.89	0.018	0.06	4.8	0.55
	Rainfed	0.95	0.94	0.023	0.07	6.2	0.49

Notes:  $b_0$  is the regression coefficient forced to the origin;  $R^2$  is the determination coefficient of the ordinary least squares regression; RMSE is the root mean square error; NRMSE is the normalized root mean square error; ARE is the average relative error; and EF is the modeling efficiency.

**Table 6.** Standard and calibrated basal crop coefficients ( $K_{cb}$ ), depletion fractions for no stress ( $p$ ), and parameters characterizing the soil evaporation layer, deep percolation and runoff.

Parameters	Initial (Default)	Calibrated
Crop	$K_{cb \text{ ini}}$	0.15
	$K_{cb \text{ mid}}$	1.15
	$K_{cb \text{ end}}$	0.35
	$p \text{ ini}$	0.55
	$p \text{ dev}$	0.55
	$p \text{ mid}$	0.50
	$p \text{ end}$	0.75
Soil evaporation	REW (mm)	12
	TEW (mm)	30
	$Z_e$ (m)	0.10
Deep percolation	$a_D$	370/360 *
	$b_D$	−0.017
Runoff	CN	85

Notes: REW and TEW are the readily and total evaporable water, respectively;  $Z_e$  is the depth of the soil evaporation layer; CN is the curve number; and  $a_D$  and  $b_D$  are the parameters of the deep percolation equation [46]. \* different values were obtained due to the spatial heterogeneity of the soil.

The calibrated potential  $K_{cb \text{ mid}} = 1.05$  (Table 6) equals that obtained by Rosa et al. [48] for Portugal. Slightly higher values, up to 1.15, are reported in other studies [20,28,39,57,58]. Differently, a smaller  $K_{cb \text{ mid}}$  was reported by Stricevic et al. [59]. The value of the  $K_{cb \text{ end}}$  depends upon crop management and its value is slightly lower than the one proposed by Allen et al. [20] because maize was harvest at low grain moisture. The  $p$  values are similar to those tabled by Allen et al. [20] except  $p$  at end season (0.75) because a large soil water depletion was intended by then.

The results above indicate that SIMDualKc is appropriate for further use in Uruguay and that the calibrated parameters are likely appropriate for being used as default ones in further applications; nevertheless, relative to soil evaporation and deep percolation, parameters may need to be adjusted considering the soil characteristics of the locations where the model will be applied.

### 3.2. Crop Coefficients and ET Partitioning

As previously mentioned, the SIMDualKc model partitions ET into  $E_s$  and  $T_{c \text{ act}}$  using the dual  $K_c$  approach. Examples of results referring to the seasonal variation of the potential and actual basal crop

coefficients,  $K_{cb}$  and  $K_{cb\ act}$ , and the evaporation coefficient  $K_e$  are presented in Figure 4. In this figure, the  $K_{cb\ mid}$  values obtained through model calibration were adjusted to the actual climate conditions when the average minimum relative humidity differed from 45% and the average wind speed was different from  $2\ m\ s^{-1}$  [20]. Figure 4 also includes irrigation and precipitation depths observed, which are depicted to ease perceiving the  $K_e$  peaks, which essentially depend upon those wetting events. The  $K_{cb\ act}$  and  $K_{cb}$  curves are coincident when full irrigation (FI) was practiced in 2012–2013 (Figure 4a). The representation of wetting events help understanding why during various periods stress occurred in 2012–2013, when deficit irrigation was practiced, with  $K_{cb\ act} < K_{cb}$  in Figure 4b, which correspond to time periods when precipitation and irrigation were insufficient to satisfy the crop demand. Figure 4c shows that water stress of the rainfed crop occurred only during a brief period in the vegetative growth and maturation stages ( $K_{cb\ act} < K_{cb}$ ) because distribution of precipitation events along the maize season was favorable; thus, in 2012–2013, rainfed maize transpiration was quite high with relatively small impacts on yield. For all other treatments whose results are not shown, the  $K_{cb\ act}$  curve lays below the  $K_{cb}$  curve during the periods when water stress occurred.

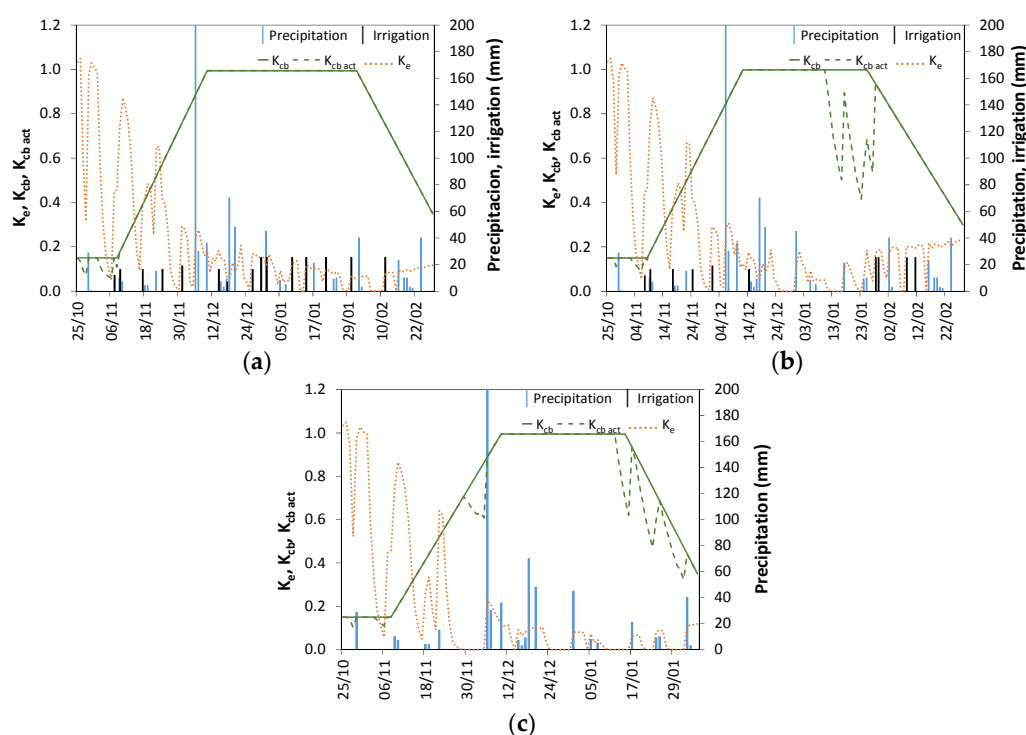


**Figure 4.** Seasonal variation of the coefficients  $K_{cb}$ ,  $K_{cb\ act}$ ,  $K_e$ , including net irrigation and precipitation for the following experimental conditions in 2012–2013: (a) FI; (b)  $DI_{FLO}$ ; and (c) rainfed.

The soil evaporation coefficient  $K_e$  presents numerous peaks in correspondence with the numerous soil wetting events as depicted in Figure 4. Peaks are larger during the initial crop growth stages, when the soil was not yet covered by the crop and more energy was available at the ground surface for evaporation. Peaks progressively decreased when the crop was growing, thus increasingly shadowing the ground.  $K_e$  peaks resulted smaller during the mid-season when the crop was fully developed and largely shadowed the ground, thus when  $f_c$  values were maximal (Table 4).  $K_e$  peaks slightly increased again during the late season when the crop senesced and  $f_c$  decreased.

The partition of  $ET_{c\ act}$  into soil evaporation and plant transpiration followed the dynamics of  $K_{cb\ act}$  and  $K_e$  discussed above. Results for  $E_s$  and  $T_{c\ act}$  for all treatments are presented in Table 7 along with other soil water balance components. For 2012–2013, when various irrigation deficits were applied, it is evident that the ratio  $E_s/T_{c\ act}$  increased with the decrease of transpiration when irrigation amounts were smaller and water deficits led to less crop development and smaller ground

cover. Results show that  $E_s$  was 22% of  $ET_{c\ act}$  in 2011–2012 and ranged from 20% to 25% of  $ET_{c\ act}$  in 2012–2013. These ratios are in agreement with those reported by other authors who used mini- and micro-lysimeters [60–62]. Much lower  $E_s/ET_{c\ act}$  ratios were reported for a drip irrigated maize with straw mulch cover [57], which supports controlling  $E_s/ET_{c\ act}$  when adopting no-till systems [4,5].

**Table 7.** Simulated water use components for drip irrigated maize, Paysandú.

Treatment	P (mm)	I (mm)	$\Delta ASW$ (mm)	DP (mm)	RO (mm)	$E_s$ (mm)	$T_{c\ act}$ (mm)	$ET_{c\ act}$ (mm)	$E_s/T_{c\ act}$ (%)	$E_s/ET_{c\ act}$ (%)
2011–2012 $DI_{FLO}$	527	275	22	104	119	133	467	600	28	22
2012–2013										
FI	701	295	−10	233	180	121	452	573	27	21
$DI_{FLO}$	701	196	10	195	175	133	404	537	33	25
$DI_{MAT}$	621	238	38	198	171	116	412	528	28	22
$DI_{VEG-FLO}$	564	170	2	103	110	120	403	523	30	23
Rainfed	613	28 *	55	133	137	87	339	426	26	20

Notes: P—precipitation; I—net irrigation;  $\Delta ASW$ —seasonal variation of available soil water; DP—deep percolation; RO—runoff;  $E_s$ —soil evaporation;  $T_{c\ act}$ —actual crop transpiration;  $ET_{c\ act}$ —actual crop evapotranspiration; \* irrigation performed to allow good crop emergence and establishment.

Results obtained for the water balance terms in Table 7 evidence the importance of the non-consumptive terms, DP and RO, which relates with the high precipitation observed and, in case of runoff, to the high depths of rainfall per event. DP represents between 18% and 33% of the seasonal precipitation and RO represents 20% to 28% of the seasonal precipitation. In case of the rainfed treatment the non-beneficial water use components (DP and RO) represented 44% of the season precipitation. Thus, despite a large fraction of rainfall water was not used by the crop, a decrease in  $T_{c\ act}$  and yield (Table 8) was observed. This yield decrease represented 35% of the  $Y_a$  observed for the FI treatment. These results show that achieving high yields is influenced by supplemental irrigation.

**Table 8.** Observed total water use (TWU), yield and water productivity.

Treatment	TWU ( $m^3$ )	$ET_{c\ act}$ (mm)	Yield ( $kg\ ha^{-1}$ )	WP ( $kg\ m^{-3}$ )	$WP_{ET}$ ( $kg\ m^{-3}$ )
2011–2012	7050	600	15,291 ( $\pm 1209$ )	2.17	2.55
2012–2013					
FI	8060	573	14,001 ( $\pm 817$ )	1.74	2.44
$DI_{FLO}$	7320	537	10,171 ( $\pm 331$ )	1.39	1.89
$DI_{MAT}$	7260	528	11,384 ( $\pm 921$ )	1.57	2.16
$DI_{VEG-FLO}$	6260	523	9167 ( $\pm 1644$ )	1.46	1.75
Rainfed	5590	426	9119 ( $\pm 1089$ )	1.63	2.14

Notes: TWU—total water use;  $ET_{c\ act}$ —crop evapotranspiration; WP—water productivity;  $WP_{ET}$ —consumptive use water productivity; in brackets the standard deviation relative to three repetitions per irrigation treatment.

The different irrigation treatments were assessed in terms of TWU and water productivity (Table 8). Results show that the highest WP value was for the year 2011–2012 ( $2.17\ kg\ m^{-3}$ ) where yields were highest and TWU was not high; the lowest WP values were obtained for the DI treatments because crop growth was impacted and yields were low (Table 8). The rainfed treatment had the lowest yield and TWU but WP is similar to that of full irrigation. WP values are similar to those reported in previous studies in Portugal [28].  $WP_{ET}$  observed values are generally superior to those reported in literature [13,14,63–65].

### 3.3. Water–Yield Relations and Yield Predictions

Pairs of actual yield-transpiration data obtained from a set of maize experiments at Paysandú were used to assess maize water yield relations. These data were available for three maize seasons and various irrigation treatments of 2010–2011, 2011–2012 and 2012–2013, some of them not analyzed above but simulated with SIMDualKc to estimate  $T_{c\ act}$  following a previous study with maize [28].

The actual yield and  $T_{c\text{ act}}$  data were used to derive the yield response factor of the model S1 (Equation (5)) and  $K_y = 1.42$  was obtained. This value is slightly larger than that obtained by Paredes et al. [28] and is in the range of values reported by Stewart et al. [12] and Kresovic et al. [26]. A slightly large value was reported by Howell et al. [66] and Payero et al. [14], while a smaller  $K_y$  was referred by Popova and Pereira [67]. Results in literature allow to consider that  $K_y = 1.42$  is likely appropriate for further use with the model S1. All yield data pairs were also used to assess the accuracy of the S2 model (Equation (6)) using the  $\beta$  values referred before (Section 2.2).

The “goodness-of-fit” indicators relative to both S1 and S2 (Table 9) allow assuming the appropriateness of parameters used for both models. The regression coefficients are close to 1.0 for both models but the  $R^2$  values are relatively low due to a large variability of observed yields. RMSE =  $1.83 \text{ t} \cdot \text{ha}^{-1}$  was obtained for S1, which represents 18% of the average observed yield ( $\bar{Y}_a$ ); RMSE was smaller for the S2 model, representing 14% of  $\bar{Y}_a$ . Results for EF, 0.59 and 0.74, respectively, for S1 and S2, indicate that the mean square error is smaller than the observed data variance.

**Table 9.** Indicators of “goodness of fit” relative to estimating maize yield using the S1 and S2 models.

Model	Parameters	$b_0$ (-)	$R^2$ (-)	RMSE ( $\text{t} \cdot \text{ha}^{-1}$ )	NRMSE (%)	ARE (%)	EF(-)
S1	$K_y = 1.42$ (this study)	1.04	0.67	1.83	17.9	17.4	0.59
	Default $K_y$ [19]	1.07	0.68	1.93	18.9	18.2	0.55
S2	$\beta_v, \beta_f$ and $\beta_m$ referred in Section 2.2	0.97	0.77	1.47	14.3	10.9	0.74
	Default $\beta_v, \beta_f$ and $\beta_m$ [12]	1.08	0.58	2.27	22.2	20.9	0.37

Notes:  $b_0$  is the regression coefficient forced to the origin;  $R^2$  is the determination coefficient of the ordinary least squares regression; RMSE is the root mean square error; NRMSE is the normalized root mean square error; ARE is the average relative error; and EF is the modeling efficiency.

Table 9 also includes the “goodness-of-fit” indicators when yield predictions used default parameters. For S1 the  $K_y$  value tabulated by Doorenbos and Kassam [19] leads acceptable but worse “goodness-of-fit” indicators, namely higher errors of estimation. For S2 the original  $\beta_v, \beta_f$  and  $\beta_m$  parameters proposed by Stewart et al. [12] lead to much worse indicators than the selected ones and the S1 model (Table 9).

Various crop growth and yield models have been tested for maize yield predictions. Stöckle et al. [52] using the CropSyst model reported RMSE representing a NRMSE of 8% to 21% of the average observed yields. Applications of the AquaCrop model show a variety of results, e.g., Heng et al. [68] reported RMSE ranging  $0.65$  to  $1.57 \text{ t} \cdot \text{ha}^{-1}$  with NRMSE of 7% to 43%, and Ahmadi et al. [16] reported RMSE of  $0.7$  and  $1.77 \text{ t} \cdot \text{ha}^{-1}$  with NRMSE of 7% and 18%. Constantin et al. [17] with AqYield and STICs models, reported NRMSE of 15% and 18% respectively. Using CERES-Maize, Lin et al. referred NRMSE near 11% [18], and Ma et al. [69] reported NRMSE ranging 6% to 12% and 5% to 7% when using, respectively, the DSAAT-CERES and the RZWQ-CERES models. Ko et al. [70] reported RMSE of  $0.5$  and  $0.87 \text{ t} \cdot \text{ha}^{-1}$  but representing NRMSE of 7% and 11% of the average observed yields. Monzon et al. [71] reported RMSE of  $1.54$  to  $2.22 \text{ t} \cdot \text{ha}^{-1}$  using CropSyst and CERES-Maize. Our results with S2 model (RMSE =  $1.47 \text{ t} \cdot \text{ha}^{-1}$  and NMRSE of 14.3%) are therefore in the range of values reported in literature, nevertheless, our approach is much less demanding than models quoted.

Overall, results above (Table 9) show that both models S1 and S2 are appropriate for predicting maize yields in further applications when using the parameters validated in this study. The S1 model should be applied when only seasonal  $T_c$  and  $T_{c\text{ act}}$  are available while the S2 model can be used when transpiration data are available for the three crop growth stages of vegetation development, flowering-pollination, and maturation.

### 3.4. Assessing Supplemental Irrigation and Rainfed Scenarios under Water Scarcity

As referred in Section 2.4, the SIMDualKc model was used with a 22-year series of weather data to estimate maize net irrigation requirements. The resulting NIR series range from 0 to 736 mm, respectively for the wettest and driest years (Figure 5). The frequently high NIR, above 370 mm,

indicate that rainfed maize may be often at risk and supplemental irrigation may be required. Thus, for the dry and very dry years, whose NIR values have the probability of non-exceedance of, respectively, 20% and 5% (Figure 5), full and deficit irrigation were assessed. Main climatic data characterizing both years are shown in Figure 6, where it is apparent that the main cause of climatic variability is precipitation while  $ET_o$  variation is relatively small.

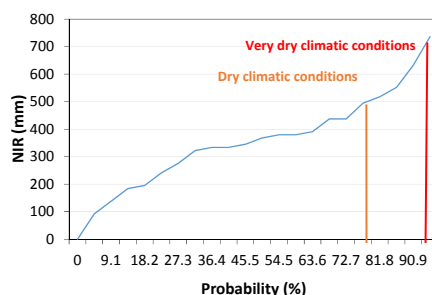


**Figure 5.** Net irrigation requirements for maize in Paysandú with identification of the dry and very dry climatic demand conditions.

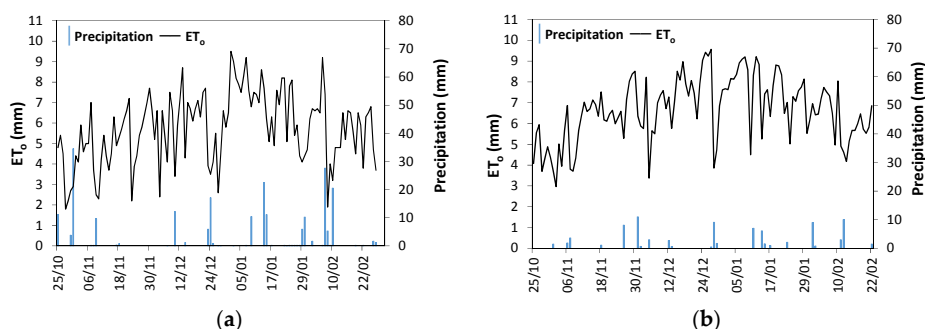


**Figure 6.** Daily precipitation and reference evapotranspiration ( $ET_o$ ) during the maize crop seasons for: (a) dry years; and (b) very dry years.

Seasonal results of the soil water balance for the considered irrigation scheduling strategies (Section 2.4) and both dry and very dry scenarios are presented in Table 10. Results show that the seasonal irrigation depth in the dry year was 71% to 84% of  $T_{c\ act}$ , respectively, for the Mod and Full irrigation scenarios; in the very dry year, it corresponded to 81 to 86% of  $T_{c\ act}$  for the same scenarios.

**Table 10.** Simulations of the soil water balance of diverse irrigation schedules for the dry and very dry years.

Data	Dry Conditions				Very Dry Conditions			
	Full	Mild	Mod	Rainfed	Full	Mild	Mod	Rainfed
Season gross irrigation (mm)	500	433	400	0	600	533	500	0
Seasonal precipitation (mm)	219				151			
RO (mm)	1	1	1	1	2	2	2	2
$\Delta ASW$ (mm)	48	73	62	88	56	61	62	79
DP (mm)	28	32	14	14	10	3	3	0
TWU (mm)	766	724	680	306	807	743	711	228
$T_{c\ act}$ (mm)	579	546	428	223	626	586	559	174
$T_c$ (mm)	581				628			
RYD (%)	1	8	14	91	1	9	15	100
$\hat{Y}_a$ ( $kg \cdot ha^{-1}$ )	13,804	12,831	12,020	1266	15,159	13,929	12,961	0
WP ( $kg \cdot m^{-3}$ )	1.80	1.77	1.77	0.41	1.88	1.87	1.82	0
$WP_{ET}$ ( $kg \cdot m^{-3}$ )	2.01	1.98	1.92	0.43	2.06	2.03	1.97	0

Notes: RO—runoff;  $\Delta ASW$ —seasonal variation of the available soil water; DP—deep percolation; TWU—total water use;  $T_c$  and  $T_{c\ act}$ —maximum and actual crop transpiration; RYD—relative yield decrease;  $\hat{Y}_a$ —estimated actual yield; WP—water productivity;  $WP_{ET}$ —consumptive use water productivity.

Adopting the improved schedules summarized in Table 10, results allow concluding that: (a) runoff may be reduced to nearly 1% of seasonal rainfall in the dry and very dry seasons; (b) deep percolation may be reduced to 2%–5% of the season water use in the dry season and less than 1% in the very dry one; however, high DP is expected to occur when very large daily rainfall depths occur; (c) small RYD are achievable but the need to cease irrigations 20 days prior to harvesting aimed at decreasing grain moisture may lead to late season water deficits causing yield decreases, particularly when maize varieties are highly sensitive to water stress; (d) computed WP and WP<sub>ET</sub> are similar to the best observed (Table 8), with highest values referring to the Full scenario in very dry conditions, which relates with achieving the highest yield, but results for the Mild deficit scenario are quite similar; and (e) WP and WP<sub>ET</sub> are higher in the very dry year because TWU is smaller than for the dry year as a decrease of rainfall may be compensated by an increase of irrigation. Results show that under dryness and/or drought conditions rainfed maize is not feasible due to very high yield losses (>91%, Table 10). This study evidences that improved schedules can lead to the best conjunctive use of rainfall and irrigation but this is only achievable when irrigation decisions are supported by a water balance model like SIMDualKc.

As previously referred, rainfed maize is commonly practiced in western Uruguay. To assess related yield consequences, following the approach by Popova et al. [6], the 22-year climatic data series were simulated for rainfed conditions and results were analyzed in terms of TWU, RYD, WP and WP<sub>ET</sub>, with the actual yield estimated with the model S2 (Equation (6)). The respective empirical probability curves for the same 22 years are presented in Figure 7.

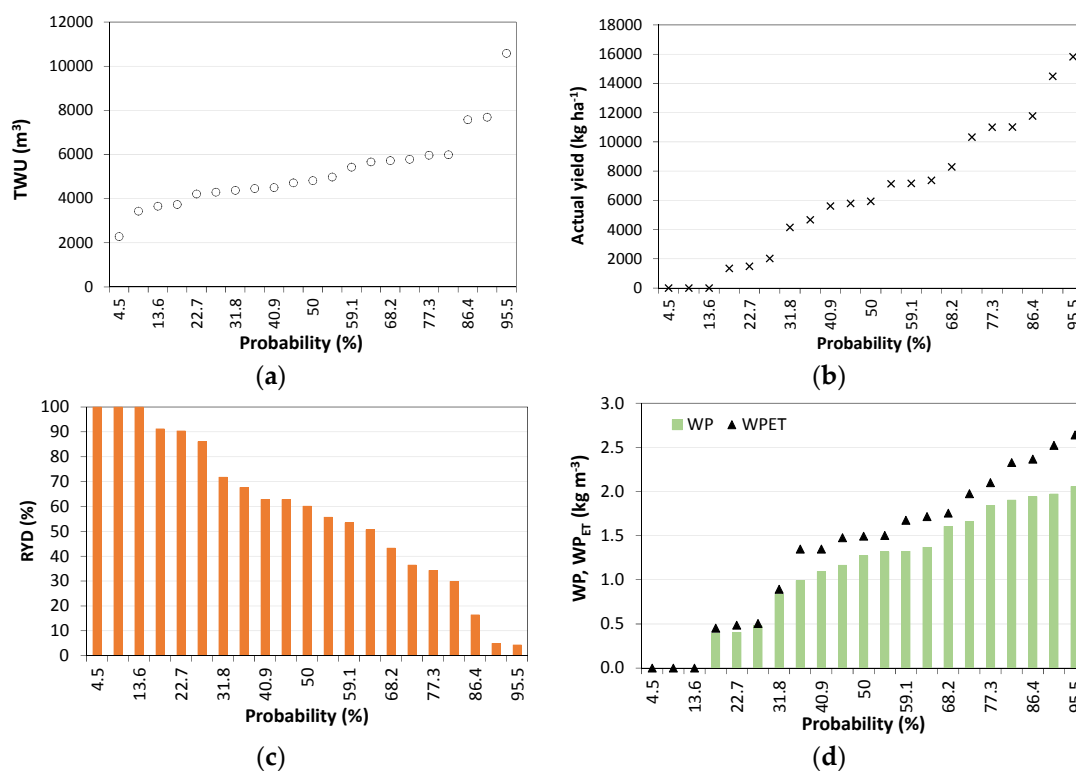


**Figure 7.** Probability curves characterizing rainfed maize through 22 years data relative to: (a) total water use (TWU); (b) estimated actual yield; (c) relative yield decrease (RYD); and (d) total and consumptive use water productivity.

TWU during the maize season ranged from 2283 to 10,585 m<sup>3</sup> (Figure 7a) reflecting the high variability of precipitation. Actual yields varied enormously (Figure 7b), from 0 to 15.8 t·ha<sup>-1</sup>; under extremely dry conditions (cf. Figure 6b), when an extreme water deficiency occurs during flowering, pollination and yield formation, grain yield could not be produced. Relative yield decreases varied

much, from just 4% in wet years to 100% in very dry years (Figure 7c) when water deficits do not allow pollinations and yield formation. It is likely that for nearly 40% of the years RYD is too much high and economic returns are insufficient; however, appropriate economic studies are required in future. WP and  $WP_{ET}$  also vary enormously (Figure 7d) due to the variability of both rainfall (and TWU, Figure 7a) and yield (Figure 7b): WP ranged from 0 to  $2.1 \text{ kg} \cdot \text{m}^{-3}$  and  $WP_{ET}$  varied from 0 to  $2.6 \text{ kg} \cdot \text{m}^{-3}$ .

#### 4. Conclusions

Field data relative to several irrigation schedules, including deficit irrigation at different crop stages, were used to calibrate and validate the water balance and irrigation scheduling model SIMDualKc by minimizing the errors of estimate of the soil water content throughout the crop seasons. The corresponding “goodness-of-fit” indicators were very good when calibrated parameters were used and also quite good when using well selected default parameters. Simulations identified well the periods when the crop was water stressed. Overall, results show that the model is appropriate for further use in Uruguay, namely to support improved irrigation scheduling practices and management. The calibrated parameters are likely appropriate for being used as default ones in further applications; nevertheless, the parameters relative to soil evaporation and deep percolation need to be adjusted considering the soil characteristics of the locations where the model will be applied.

Results have shown that the ratio  $E_s/T_{c \text{ act}}$  increased with the decrease of transpiration when water deficits limited crop development and led to reduced ground cover. The ratio  $E_s/ET_{c \text{ act}}$  behaved similarly. Results for this ratio agree well with literature. These ratios may be reduced if mulched direct planting is adopted. Non-consumptive water balance terms DP and RO were quite high due to the local rainfall regime.

Both water–yield models S1 and S2 were successfully parameterized and their test for various sets of data provided quite good “goodness-of-fit” indicators. The staged S2 model provided better predictions than the model S1 because it considers the effects of water stress during the critical crop stages. Their errors were in the range of those reported in literature for the application of more demanding crop growth and yield models. Therefore, predictions using those models may be used in the future to estimate yields required for water productivity estimations. WP results were quite high, with best values when higher yields were obtained.

Several irrigation scheduling scenarios were assessed for dry and very dry years. Respective results show that a mild deficit irrigation is likely appropriate if considering precise deficit irrigation thresholds. Modeling provided good solutions for the conjunctive use of rainfall and irrigation, with high control of RO and DP, thus leading to more efficient water use. Computed performance indicators, mainly WP and  $WP_{ET}$ , were similar to those computed when observed data were used. Results for rainfed maize have shown a great range of yield and water productivity variation, which likely lead to non-feasible rainfed production in about 40% of the years. However, a more appropriate assessment of the feasibility of rainfed and deficit irrigation solutions requires using field economic data and developing an adequate economic analysis in addition to indicators used herein.

**Acknowledgments:** The third author acknowledges the Post-Doctoral research grant (SFRH/BPD/102478/2014) awarded by the Foundation for Science and Technology, Portugal.

**Author Contributions:** The first author contributed for the current study by developing the field experiments and related data analysis, testing the model application, and writing the present manuscript. The second author was responsible for supervising the experimental study. The third author contributed by supporting the use of SIMDualKc modeling, testing the modeling approaches and supporting the manuscript writing. The senior author was responsible for theory and practice of evapotranspiration and water balance and for directing manuscript writing.

**Conflicts of Interest:** The authors declare no conflict of interest.

## References

1. Redo, D.J.; Aide, T.M.; Clark, M.L.; Andrade-Núñez, M.J. Impacts of internal and external policies on land change in Uruguay, 2001–2009. *Environ. Conserv.* **2012**, *39*, 122–131. [[CrossRef](#)]
2. Giménez, L. Production of corn with water stress at different stages of development. *Agrociencia* **2012**, *16*, 92–102. (In Spanish)
3. Frank, F.C.; Viglizzo, E.F. Water use in rain-fed farming at different scales in the Pampas of Argentina. *Agric. Syst.* **2012**, *109*, 35–42. [[CrossRef](#)]
4. García-Préchac, F.; Ernst, O.; Siri-Prieto, G.; Terra, J.A. Integrating no-till into crop-pasture rotations in Uruguay. *Soil Till. Res.* **2004**, *77*, 1–13. [[CrossRef](#)]
5. Wingeyer, A.B.; Amado, T.J.C.; Pérez-Bidegain, M.; Studdert, G.A.; Varela, C.H.P.; Garcia, F.O.; Karlen, D.L. Soil quality impacts of current South American agricultural practices. *Sustainability* **2015**, *7*, 2213–2242. [[CrossRef](#)]
6. Popova, Z.; Ivanova, M.; Martins, D.; Pereira, L.S.; Doneva, K.; Alexandrov, V.M.; Kercheva, M. Vulnerability of Bulgarian agriculture to drought and climate variability with focus on rainfed maize systems. *Nat. Hazards* **2014**, *74*, 865–886. [[CrossRef](#)]
7. Pereira, L.S.; Oweis, T.; Zairi, A. Irrigation management under water scarcity. *Agric. Water Manag.* **2002**, *57*, 175–206. [[CrossRef](#)]
8. Pereira, L.S.; Cordery, I.; Iacovides, I. Improved indicators of water use performance and productivity for sustainable water conservation and saving. *Agric. Water Manag.* **2012**, *108*, 39–51. [[CrossRef](#)]
9. Molden, D.; Oweis, T.; Steduto, P.; Bindraban, P.; Hanjra, M.A.; Kijne, J. Improving agricultural water productivity: Between optimism and caution. *Agric. Water Manag.* **2010**, *97*, 528–535. [[CrossRef](#)]
10. Lankford, B. Fictions, fractions, factorials and fractures; On the framing of irrigation efficiency. *Agric. Water Manag.* **2012**, *108*, 27–38. [[CrossRef](#)]
11. Oweis, T.; Hachum, A. Optimizing supplemental irrigation: Tradeoffs between profitability and sustainability. *Agric. Water Manag.* **2009**, *96*, 511–516. [[CrossRef](#)]
12. Stewart, J.I.; Hagan, R.M.; Pruitt, W.O.; Danielson, R.E.; Franklin, W.T.; Hanks, R.J.; Riley, J.P.; Jackson, E.B. *Optimizing Crop Production Through Control of Water and Salinity Levels in the Soil*; Utah Water Research Laboratory: Logan, UT, USA, 1977; p. 191.
13. Payero, J.O.; Melvin, S.R.; Irmak, S.; Tarkalson, D. Yield response of corn to deficit irrigation in a semiarid climate. *Agric. Water Manag.* **2006**, *84*, 101–112. [[CrossRef](#)]
14. Payero, J.O.; Tarkalson, D.D.; Irmak, S.; Davison, D.; Petersen, J.L. Effect of timing of a deficit-irrigation allocation on corn evapotranspiration, yield, water use efficiency and dry mass. *Agric. Water Manag.* **2009**, *96*, 1387–1397. [[CrossRef](#)]
15. Kloss, S.; Pushpalatha, R.; Kamoyo, K.J.; Schütze, N. Evaluation of crop models for simulating and optimizing deficit irrigation systems in arid and semi-arid countries under climate variability. *Water Resour. Manag.* **2012**, *26*, 997–1014. [[CrossRef](#)]
16. Ahmadi, S.H.; Mosallaeepour, E.; Kamgar-Haghighi, A.A.; Sepaskhah, A.R. Modeling maize yield and soil water content with Aquacrop under full and deficit irrigation managements. *Water Resour. Manag.* **2015**, *29*, 2837–2853. [[CrossRef](#)]
17. Constantin, J.; Willaume, M.; Murgue, C.; Lacroix, B.; Therond, O. The soil-crop models STICS and AqYield predict yield and soil water content for irrigated crops equally well with limited data. *Agric. For. Meteorol.* **2015**, *206*, 55–68. [[CrossRef](#)]
18. Lin, Y.; Wua, W.; Gea, Q. CERES-Maize model-based simulation of climate change impacts on maize yields and potential adaptive measures in Heilongjiang Province, China. *J. Sci. Food Agric.* **2015**, *95*, 2838–2849. [[CrossRef](#)] [[PubMed](#)]
19. Doorenbos, J.; Kassam, A.H. *Yield Response to Water*; FAO Irrigation and Drainage Paper 33; FAO: Rome, Italy, 1979; p. 193.
20. Allen, R.G.; Pereira, L.S.; Raes, D.; Smith, M. *Crop. Evapotranspiration. Guidelines for Computing Crop. Water Requirements*; FAO Irrigation and Drainage Paper 56; FAO: Rome, Italy, 1998; p. 300.
21. Steduto, P.; Hsiao, T.C.; Fereres, E.; Raes, D., Eds.; *Crop. Yield Response to Water*; FAO Irrigation and Drainage Paper 66; FAO: Rome, Italy, 2012; p. 500.

22. Garg, N.K.; Dadhich, S.M. Integrated non-linear model for optimal cropping pattern and irrigation scheduling under deficit irrigation. *Agric. Water Manag.* **2014**, *140*, 1–13. [[CrossRef](#)]
23. Leite, K.N.; Martínez-Romero, A.; Tarjuelo, J.M.; Domínguez, A. Distribution of limited irrigation water based on optimized regulated deficit irrigation and typical meteorological year concepts. *Agric. Water Manag.* **2015**, *148*, 164–176. [[CrossRef](#)]
24. Yu, Y.; Disse, M.; Yu, R.; Yu, G.; Sun, L.; Huttner, P.; Rumbau, C. Large-scale hydrological modeling and decision-making for agricultural water consumption and allocation in the main stem Tarim River, China. *Water* **2015**, *7*, 2821–2839. [[CrossRef](#)]
25. Irmak, S. Interannual variation in long-term center pivot—Irrigated maize evapotranspiration and various water productivity response indices. I: Grain yield, actual and basal evapotranspiration, irrigation-yield production functions, evapotranspiration-yield production functions, and yield response factors. *J. Irrig. Drain. Eng.* **2015**. [[CrossRef](#)]
26. Kresović, B.; Tapanarova, A.; Tomić, Z.; Zivoti, L.; Vujović, D.; Sredojević, Z.; Gajić, B. Grain yield and water use efficiency of maize as influenced by different irrigation regimes through sprinkler irrigation under temperate climate. *Agric. Water Manag.* **2016**, *169*, 34–43. [[CrossRef](#)]
27. Li, Z.; Sun, Z. Optimized single irrigation can achieve high corn yield and water use efficiency in the Corn Belt of Northeast China. *Eur. J. Agron.* **2016**, *75*, 12–24. [[CrossRef](#)]
28. Paredes, P.; Rodrigues, G.C.; Alves, I.; Pereira, L.S. Partitioning evapotranspiration, yield prediction and economic returns of maize under various irrigation management strategies. *Agric. Water Manag.* **2014**, *135*, 27–39. [[CrossRef](#)]
29. Grafton, R.Q.; Chu, H.L.; Stewardson, M.; Kompas, T. Optimal dynamic water allocation: Irrigation extractions and environmental tradeoffs in the Murray River, Australia. *Water Resour. Res.* **2011**, *47*, W00G08. [[CrossRef](#)]
30. Parsinejad, M.; Yazdi, A.B.; Araghinejad, S.; Nejadhashemi, A.P.; Tabrizi, M.S. Optimal water allocation in irrigation networks based on real time climatic data. *Agric. Water Manag.* **2013**, *117*, 1–8. [[CrossRef](#)]
31. Sadati, S.K.; Speelman, S.; Sabouhi, M.; Gitizadeh, M.; Ghahraman, B. Optimal irrigation water allocation using a genetic algorithm under various weather conditions. *Water* **2014**, *6*, 3068–3084. [[CrossRef](#)]
32. Abi Saab, M.T.; Albrizio, R.; Nangia, V.; Karam, F.; Roupheal, Y. Developing scenarios to assess sunflower and soybean yield under different sowing dates and water regimes in the Bekaa valley (Lebanon): Simulations with Aquacrop. *Int. J. Plant. Prod.* **2014**, *8*, 457–482.
33. González-Perea, R.; Camacho-Poyato, E.; Montesinos, P.; Rodríguez-Díaz, J.A. Optimization of irrigation scheduling using soil water balance and genetic algorithms. *Water Resour. Manag.* **2016**. [[CrossRef](#)]
34. Rosa, R.D.; Paredes, P.; Rodrigues, G.C.; Alves, I.; Fernando, R.M.; Pereira, L.S.; Allen, R.G. Implementing the dual crop coefficient approach in interactive software. 1. Background and computational strategy. *Agric. Water Manag.* **2012**, *103*, 8–24. [[CrossRef](#)]
35. Kottke, M.; Grieser, J.; Beck, C.; Rudolf, B.; Rubel, F. World Map of the Köppen-Geiger climate classification updated. *Meteorol. Z.* **2006**, *15*, 259–263. [[CrossRef](#)]
36. Gardner, W.H. Water content. In *Methods of Soil Analysis. Part. 1. Physical and Mineralogical Methods*, 2nd ed.; Klute, A., Ed.; American Society of Agronomy and Soil Science Society of America: Madison, WI, USA, 1986; pp. 493–544.
37. Echarte, L.; Luque, S.; Andrade, F.H.; Sadras, V.O.; Cirilo, A.; Otegui, M.E.; Vega, C.R.C. Response of maize kernel number to plant density in Argentinean hybrids released between 1965 and 1993. *Field Crop. Res.* **2000**, *68*, 1–8. [[CrossRef](#)]
38. Zhao, N.N.; Liu, Y.; Cai, J.B.; Rosa, R.; Paredes, P.; Pereira, L.S. Dual crop coefficient modelling applied to the winter wheat—Summer maize crop sequence in North China Plain: Basal crop coefficients and soil evaporation component. *Agric. Water Manag.* **2013**, *117*, 93–105. [[CrossRef](#)]
39. Allen, R.G.; Pereira, L.S.; Smith, M.; Raes, D.; Wright, J.L. FAO-56 Dual crop coefficient method for estimating evaporation from soil and application extensions. *J. Irrig. Drain. Eng.* **2005**, *131*, 2–13. [[CrossRef](#)]
40. Paço, T.A.; Pôças, I.; Cunha, M.; Silvestre, J.C.; Santos, F.L.; Paredes, P.; Pereira, L.S. Evapotranspiration and crop coefficients for a super intensive olive orchard. An application of SIMDualKc and METRIC models using ground and satellite observations. *J. Hydrol.* **2014**, *519*, 2067–2080. [[CrossRef](#)]
41. Qiu, R.; Du, T.; Kang, S.; Chen, R.; Wu, L. Assessing the SIMDualKc model for estimating evapotranspiration of hot pepper grown in a solar greenhouse in Northwest China. *Agric. Syst.* **2015**, *138*, 1–9. [[CrossRef](#)]

42. Ding, R.; Kang, S.; Zhang, Y.; Hao, X.; Tong, L.; Du, T. Partitioning evapotranspiration into soil evaporation and transpiration using a modified dual crop coefficient model in irrigated maize field with ground-mulching. *Agric. Water Manag.* **2013**, *127*, 85–96. [[CrossRef](#)]
43. Kool, D.; Agam, N.; Lazarovitch, N.; Heitman, J.L.; Sauer, T.J.; Ben-Gal, A. A review of approaches for evapotranspiration partitioning. *Agric. For. Meteorol.* **2014**, *184*, 56–70. [[CrossRef](#)]
44. Ritchie, J.T. Model for predicting evaporation from a row crop with incomplete cover. *Water Resour. Res.* **1972**, *8*, 1204–1213. [[CrossRef](#)]
45. Allen, R.G.; Wright, J.L.; Pruitt, W.O.; Pereira, L.S.; Jensen, M.E. Water requirements. In *Design and Operation of Farm. Irrigation Systems*, 2nd ed.; Hoffman, G.J., Evans, R.G., Jensen, M.E., Martin, D.L., Elliot, R.L., Eds.; ASABE: St. Joseph, MI, USA, 2007; pp. 208–288.
46. Liu, Y.; Pereira, L.S.; Fernando, R.M. Fluxes through the bottom boundary of the root zone in silty soils: Parametric approaches to estimate groundwater contribution and percolation. *Agric. Water Manag.* **2006**, *84*, 27–40. [[CrossRef](#)]
47. Doorenbos, J.; Pruitt, W.O. *Guidelines for Predicting Crop. Water Requirements*; FAO Irrigation and Drainage Paper 24; FAO: Rome, Italy, 1977; p. 179.
48. Rosa, R.D.; Paredes, P.; Rodrigues, G.C.; Fernando, R.M.; Alves, I.; Pereira, L.S.; Allen, R.G. Implementing the dual crop coefficient approach in interactive software. 2. Model testing. *Agric. Water Manag.* **2012**, *103*, 62–77. [[CrossRef](#)]
49. Pereira, L.S.; Paredes, P.; Rodrigues, G.C.; Neves, M. Modeling malt barley water use and evapotranspiration partitioning in two contrasting rainfall years. Assessing AquaCrop and SIMDualKc models. *Agric. Water Manag.* **2015**, *159*, 239–254. [[CrossRef](#)]
50. Wu, Y.; Liu, T.; Paredes, P.; Duan, L.; Pereira, L.S. Water use by a groundwater dependent maize in a semi-arid region of Inner Mongolia: Evapotranspiration partitioning and capillary rise. *Agric. Water Manag.* **2015**, *152*, 222–232. [[CrossRef](#)]
51. Sinclair, T.R.; Tanner, C.B.; Bennett, J.M. Water-use efficiency in crop production. *BioScience* **1984**, *34*, 36–40.
52. Stöckle, C.O.; Donatelli, M.; Nelson, R. CropSyst, a cropping systems simulation model. *Eur. J. Agron.* **2003**, *18*, 289–307. [[CrossRef](#)]
53. Alves, I.; Fontes, J.C.; Pereira, L.S. Water-yield relations for corn. In *Planning, Operation, and Management of Irrigation Systems for Water and Energy Conservation*; Proc. Special Tech. Session. Chinese Nat.Com. ICID: Beijing, China, 1991; Volume I-A, pp. 154–161.
54. Legates, D.; McCabe, G., Jr. Evaluating the use of goodness of fit measures in hydrologic and hydroclimatic model validation. *Water Resour. Res.* **1999**, *35*, 233–241. [[CrossRef](#)]
55. Nash, J.E.; Sutcliffe, J.V. River flow forecasting through conceptual models: Part 1. A discussion of principles. *J. Hydrol.* **1970**, *10*, 282–290. [[CrossRef](#)]
56. García-Petillo, M. Critical analysis of the drip irrigation method under the conditions of Uruguay. *Agrociencia* **2010**, *14*, 36–43. (In Spanish)
57. Martins, J.D.; Rodrigues, G.C.; Paredes, P.; Carlesso, R.; Oliveira, Z.B.; Knies, A.; Petry, M.T.; Pereira, L.S. Dual crop coefficients for full and deficit irrigated maize in southern Brazil: Model calibration and validation for sprinkler and drip irrigation and mulched soil. *Biosyst. Eng.* **2013**, *115*, 291–310. [[CrossRef](#)]
58. González-Dugo, M.P.; Neale, C.M.U.; Mateos, L.; Kustas, W.P.; Prueger, J.H.; Anderson, M.C.; Li, F. A comparison of operational remote sensing-based models for estimating crop evapotranspiration. *Agric. For. Meteorol.* **2009**, *149*, 1843–1853. [[CrossRef](#)]
59. Stricevic, R.; Cosic, M.; Djurovic, N.; Pejic, B.; Maksimovic, L. Assessment of the FAO AquaCrop model in the simulation of rainfed and supplementally irrigated maize, sugar beet and sunflower. *Agric. Water Manag.* **2011**, *98*, 1615–1621. [[CrossRef](#)]
60. Klocke, N.L.; Todd, R.W.; Schneekloth, J.P. Soil water evaporation in irrigated corn. *Appl. Eng. Agric.* **1996**, *12*, 301–306. [[CrossRef](#)]
61. Kang, S.; Gu, B.; Du, T.; Zhang, J. Crop coefficient and ratio of transpiration to evapotranspiration of winter wheat and maize in a semi-humid region. *Agric. Water Manag.* **2003**, *59*, 239–254. [[CrossRef](#)]
62. Tahiri, A.Z.; Anyoji, H.; Yasuda, H. Fixed and variable light extinction coefficients for estimating plant transpiration and soil evaporation under irrigated maize. *Agric. Water Manag.* **2006**, *84*, 186–192. [[CrossRef](#)]

63. Hernández, M.; Echarte, L.; Della Maggiora, A.; Cambareri, M.; Barbieri, P.; Cerrudo, D. Maize water use efficiency and evapotranspiration response to N supply under contrasting soil water availability. *Field Crops Res.* **2015**, *178*, 8–15. [[CrossRef](#)]
64. Zwart, S.J.; Bastiaanssen, W.G.M. Review of measured crop water productivity values for irrigated wheat, rice, cotton and maize. *Agric. Water Manag.* **2004**, *69*, 115–133. [[CrossRef](#)]
65. Aydinsakir, K.; Erdal, S.; Buyuktas, D.; Bastug, R.; Toker, R. The influence of regular deficit irrigation applications on water use, yield, and quality components of two corn (*Zea. mays* L.) genotypes. *Agric. Water Manag.* **2013**, *128*, 65–71. [[CrossRef](#)]
66. Howell, T.A.; Schneider, A.D.; Evett, S.R. Surface and subsurface microirrigation of corn-Southern High Plains. *Trans. ASAE* **1997**, *40*, 635–641. [[CrossRef](#)]
67. Popova, Z.; Pereira, L.S. Modelling for maize irrigation scheduling using long term experimental data from Plovdiv region, Bulgaria. *Agric. Water Manag.* **2011**, *98*, 675–683. [[CrossRef](#)]
68. Heng, L.K.; Hsiao, T.; Evett, S.; Howell, T.; Steduto, P. Validating the FAO AquaCrop model for irrigated and water deficient field maize. *Agron. J.* **2009**, *101*, 488–498. [[CrossRef](#)]
69. Ma, L.; Hoogenboom, G.; Ahuja, L.R.; Ascough, J.C., II; Saseendran, S.A. Evaluation of the RZWQM-CERES-Maize hybrid model for maize production. *Agric. Syst.* **2006**, *87*, 274–295. [[CrossRef](#)]
70. Ko, J.; Piccinni, G.; Steglich, E. Using EPIC model to manage irrigated cotton and maize. *Agric. Water Manag.* **2009**, *96*, 1323–1331. [[CrossRef](#)]
71. Monzon, J.P.; Sadras, V.O.; Andrade, F.H. Modelled yield and water use efficiency of maize in response to crop management and Southern Oscillation Index in a soil-climate transect in Argentina. *Field Crop. Res.* **2012**, *130*, 8–18. [[CrossRef](#)]



© 2016 by the authors; licensee MDPI, Basel, Switzerland. This article is an open access article distributed under the terms and conditions of the Creative Commons Attribution (CC-BY) license (<http://creativecommons.org/licenses/by/4.0/>).